Chapter 1

Complex dynamic behavior on transition in a solid combustion model

Jun Yu
The University of Vermont
jun@cems.uvm.edu
Laura K. Gross
The University of Akron
gross@math.uakron.edu
Christopher M. Danforth
The University of Vermont
chris.danforth@uvm.edu

Through examples in a free-boundary model of solid combustion, this study concerns nonlinear transition behavior of small disturbances of front propagation and temperature as they evolve in time. This includes complex dynamics of period doubling, quadrupling, and six-folding, and it eventually leads to chaotic oscillations. The mathematical problem is interesting as solutions to the linearized equations are unstable when a bifurcation parameter related to the activation energy passes through a critical value. Therefore, it is crucial to account for the cumulative effect of small nonlinearities to obtain a correct description of the evolution over long times. Both asymptotic and numerical solutions are studied. We show that for special parameters our method with some dominant modes captures the formation of coherent structures. Weakly nonlinear analysis for a general case is difficult because of the complex dynamics of the problem, which lead to chaos. We discuss possible methods to improve our prediction of the solutions in the chaotic case.

1.1 Introduction

We study the nonuniform dynamics of front propagation in solid combustion: a chemical reaction that converts a solid fuel directly into solid products with no intermediate gas phase formation. For example, in self-propagating high-temperature synthesis (SHS), a flame wave advancing through powdered ingredients leaves high-quality ceramic materials or metallic alloys in its wake. (See, for instance, [7].)

The propagation results from the interplay between heat generation and heat diffusion in the medium. A balance exists between the two in some parametric regimes, producing a constant burning rate. In other cases, competition between reaction and diffusion results in a wide variety of nonuniform behaviors, some leading to chaos.

In studying the nonlinear transition behavior of small disturbances of front propagation and temperature as they evolve in time, we compare quantitatively the results of weakly nonlinear analysis with direct simulations. We also propose techniques for the accurate simulation of chaotic solutions.

1.2 Mathematical analysis

We use a version of the sharp-interface model of solid combustion introduced by Matkowsky and Sivashinsky [6]. It includes the heat equation on a semi-infinite domain and a nonlinear kinetic condition imposed on the moving boundary.

Specifically, we seek the temperature distribution $u(x,t)$ in one spatial dimension and the interface position $\Gamma(t) = \{x | x = f(t)\}$ that satisfy the appropriately non-dimensionalized free-boundary problem

$$\frac{\partial u}{\partial t} = \frac{\partial^2 u}{\partial x^2}, \quad x > f(t), \quad t > 0, \tag{1.1}$$

$$V = G\left(u\big|_\Gamma\right), \quad t > 0, \tag{1.2}$$

$$\left.\frac{\partial u}{\partial x}\right|_\Gamma = -V, \quad t > 0. \tag{1.3}$$

Here V is the velocity of the rightward-traveling interface, i.e. $V = df/dt$. In addition, the temperature satisfies the condition $u \to 0$ as $x \to \infty$; that is, the ambient temperature is normalized to zero at infinity.

To model solid combustion, we take the Arrhenius function as the kinetics function G in the non-equilibrium interface condition (1.2) [1, 8]. Then, with appropriate nondimensionalization, the velocity of propagation relates to the interface temperature as:

$$V = \exp\left[\left(\frac{1}{\nu}\right)\frac{u-1}{\sigma + (1-\sigma)u}\right] \tag{1.4}$$

at the interface Γ. Here ν is inversely proportional to the activation energy of the exothermic chemical reaction that occurs at the interface, and $0 < \sigma < 1$

is the ambient temperature nondimensionalized by the adiabatic temperature of combustion products. (See [3].)

The free-boundary problem admits a traveling-wave solution

$$u(x,t) = \exp(-x+t), \quad f(t) = t. \tag{1.5}$$

It is linearly unstable when ν is less than the critical value $\nu_c = 1/3$. (See, for example, [4, 10].)

For the weakly nonlinear analysis, let ϵ^2 be a small deviation from the neutrally stable value of ν, namely

$$\epsilon^2 = \nu_c - \nu = \frac{1}{3} - \nu. \tag{1.6}$$

We perturb the basic solution (1.5) by ϵ times the most linearly unstable mode, evaluated at both the neutrally stable parameter value $\nu = 1/3$ and the corresponding neutrally stable eigenvalue, together with complex-conjugate terms. In the velocity expansion, we also include ϵ times the constant solution to the linearized problem (although we do not mention it explicitly in the sequel). See [5].

The normal-mode perturbation is modulated by a complex-valued, slowly varying amplitude function $A(\tau)$, where $\tau = \epsilon^2 t$. The amplitude envelope satisfies the solvability condition

$$\frac{dA}{d\tau} = \chi A + \beta A^2 \bar{A}, \tag{1.7}$$

where χ and β are complex constants. (See [5] for details.)

The evolution equation (1.7) has circular limit cycles in the complex-A plane for all values of the kinetic parameter σ in the interval $0 < \sigma < 1$ (i.e. for all physical values of σ). To find $A(\tau)$, we integrate the ordinary differential equation (1.7) using a fourth-order Runge-Kutta method.

1.3 Results and discussion

To compare quantitatively the asymptotics with numerics, we first consider $\epsilon = 0.1$. The value of ν remains at the marginally unstable value $\nu_c - \epsilon^2$, as in equation (1.6), so $\nu \approx 0.32\bar{3}$. We show in this section that this choice of ϵ corresponds to a mix of dynamics as σ varies. Subsequently, we comment on the impact on the front behavior of both decreasing and increasing ϵ.

To start, take $\sigma = 0.48$ in the kinetics function (1.4). For the remainder of this paper we take the initial condition $A(0) = 0.1$, unless otherwise indicated.

Figure 1.1 shows the numerical (solid line) and asymptotic (dashed line) values of front speed perturbation as a function of time t in the interval $0 \le t \le 60$. To find the numerical solution, we used the Crank-Nicolson method to solve the problem in a front-attached coordinate frame, reformulating the boundary condition (1.3) for robustness. (See [5] for details.) As for the asymptotic

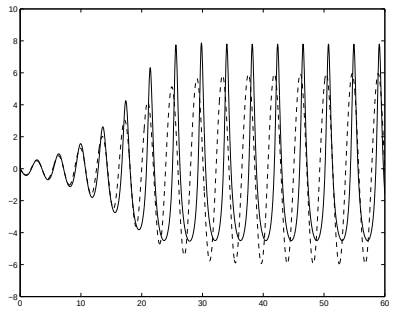

Figure 1.1: Velocity perturbation versus time: comparison between numerical (solid line) and asymptotic (dashed line) for Arrhenius kinetics, $\sigma = 0.48$, $\epsilon = 0.1$, $A(0) = 0.1$ ($\nu \approx \nu_c - \epsilon^2 = 1/3 - (0.1)^2 = 0.32\overline{3}$)

solution, the previous section describes the order-ϵ perturbation to the traveling-wave solution (1.5). In the figure we have additionally included an order-ϵ^2 correction.

Figure 1.1 reveals that from $t = 0$ to about $t = 30$, the small front speed perturbation is linearly unstable, and its amplitude grows exponentially in time. As this amplitude becomes large, nonlinearity takes effect. At around $t = 30$, the front speed perturbation has reached steady oscillation. The asymptotic solution accurately captures the period in both transient behavior for $t = 0$ to 30 and the long-time behavior after $t = 30$. The amplitude and phase differ somewhat. This is an example in which the weakly nonlinear approach describes well the marginally unstable large-time behaviors: A single modulated temporal mode captures the dynamics.

To identify additional such regimes systematically, we calculate numerically the velocity perturbation data on the time interval $35 < t < 85$, throughout the range of physical values of the kinetics parameter σ (i.e. $0 < \sigma < 1$). Figure 1.2 summarizes the Fourier transformed velocity data. For each σ value and each frequency, the color indicates the corresponding amplitude, with the red end of the spectrum standing for larger numbers than the violet end. For roughly $0.3 < \sigma < 0.6$, the figure shows the dominance of the lowest-order mode, suggesting the appropriateness of the weakly nonlinear analysis in this range. For other values of σ, a single mode cannot be expected to capture the full dynamics of the solution.

In particular, when σ is greater than approximately 0.6, solutions have sharp peaks, even sharper than the numerical solution in Figure 1.1. Figure 1.2 shows that when σ is smaller than approximately 0.3, the Fourier spectrum has a complicated character, starting with the emergence of a period-doubling solution for $\sigma \approx 0.25$. Figure 1.3 gives a closer look at the dominant modes for the case of small σ; notice the bifurcation to a six-folding solution near $\sigma = 0.201$. The four numerical solutions in Figures 1.4 and 1.5 illustrate the cascade of period-replicating solutions, including doubling ($\sigma = 0.22$), quadrupling ($\sigma = 0.21$),

and six-folding ($\sigma = 0.20075$). Note that Figure 1.2 reflects the breakdown of the numerical solution for σ less than approximately 0.15.

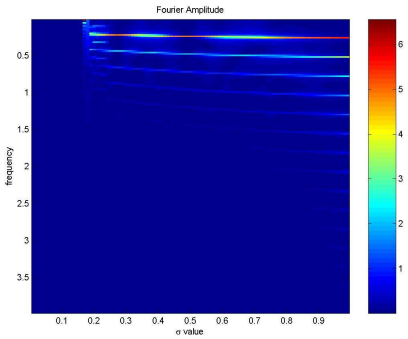

Figure 1.2: Amplitudes corresponding to each frequency of the Fourier transformed velocity perturbation data for the Arrhenius kinetics parameter σ in the interval $(0, 1)$, $\epsilon = 0.1$, $A(0) = 0.1$, $35 < t < 85$ ($\nu \approx \nu_c - \epsilon^2 = 1/3 - (0.1)^2 = 0.32\bar{3}$)

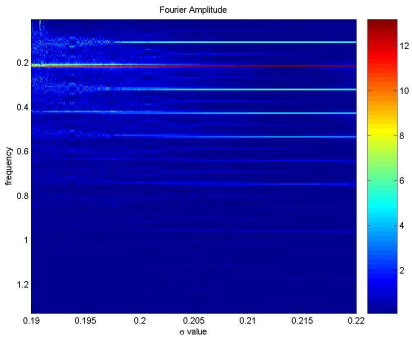

Figure 1.3: Amplitudes corresponding to each frequency of the Fourier transformed velocity perturbation data for the Arrhenius kinetics parameter σ in the interval $(0.19, 0.22)$, $\epsilon = 0.1$, $A(0) = 0.1$, $35 < t < 85$ ($\nu \approx \nu_c - \epsilon^2 = 1/3 - (0.1)^2 = 0.32\bar{3}$)

The cascade of period-replicating solutions for decreasing σ leads to chaos. Figure 1.6 (corresponding to $\sigma = 0.185$) shows the sensitivity of the velocity perturbation to initial conditions. In the figure, note that from $t = 0$ to approximately $t = 25$, the small front speed perturbation is linearly unstable, and its amplitude grows exponentially in time, similar to the profile in Figure 1.1. As the amplitude becomes large, nonlinearity again comes into play. Still, the curves corresponding to two initial conditions (one with $A(0) = 0.1$ and the other with $A(0) = 0.1000001$) remain indistinguishable for a long time. However, as time approaches 100 the two profiles begin to diverge, and as time evolves past 120 they disagree wildly.

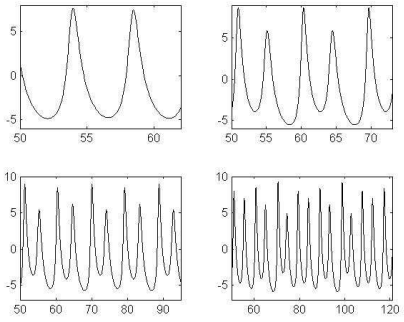

Figure 1.4: Velocity perturbations versus time ($\epsilon = 0.1$, $A(0) = 0.1$, $\nu \approx \nu_c - \epsilon^2 = 1/3 - (0.1)^2 = 0.32\overline{3}$) clockwise from upper left: periodic solution for $\sigma = 0.48$ (cf. Figure 1.1), period doubling ($\sigma = 0.22$), period quadrupling ($\sigma = 0.21$), period six-folding ($\sigma = 0.20075$)

We propose a couple of techniques to improve model predictions in the chaotic case. One–ensemble forecasting–requires the generation of velocity profiles that correspond to slightly different initial conditions. The degree of agreement among curves in the collection (ensemble) demonstrates the level of reliability of predictions. In the spirit of the jet-stream forecasts in [9], additional data can be provided at the points at which the individual members of the ensemble diverge. For example, Figure 1.6, which shows an "ensemble" of only two curves, gives a preliminary indication of the need for more data at $t = 100$.

Alternatively, we can more accurately represent solid combustion by using statistical methods to "train" the model. Comparisons with experimental data can reveal systematic and predictable error, as in Figure 1.7 (courtesy of [2]). The figure, which provides an analogy to the problem under consideration, shows that temperature forecasts near the sea surface off the coast of Japan are typically too warm [2]. That is, the actual temperatures minus the predicted temperatures are negative values, represented as yellow, blue, and violet in the figure. In describing combustion, as in describing sea temperatures, one can compensate methodically for such error.

As the bifurcation parameter ν approaches ever closer to the neutrally stable value (i.e. as ϵ decreases), the complex dynamics—including chaos—disappear. For example, when $\epsilon = 0.06$, the asymptotic and numerical solutions agree closely throughout the physical range of σ ($0 < \sigma < 1$). By contrast, when ϵ grows to 0.12, the σ interval in which one mode dominates strongly has a length of only 0.01. Varying ϵ quantifies the domain of applicability of the weakly nonlinear analysis and delineates the role of σ in the dynamics. (See [5].)

In summary, linear instability provides a mechanism for transition to nonlinear coherent structures. Weakly nonlinear analysis allows the asymptotic study of the evolution of small disturbances during this transition, providing insight

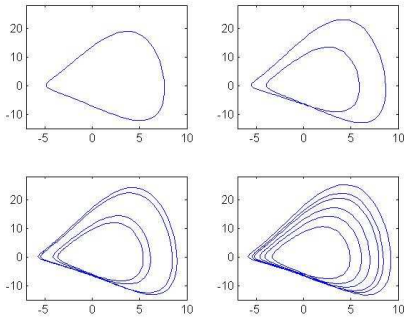

Figure 1.5: Phase plots of the four solutions in Figure 1.4: dv/dt versus velocity perturbation $v(t)$

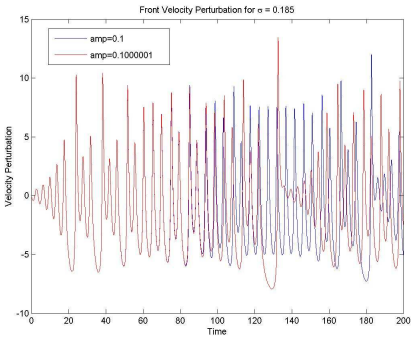

Figure 1.6: Velocity perturbation versus time: numerical solution for $\sigma = 0.185$, $\epsilon = 0.1$, $A(0) = 0.1$ and $A(0) = 0.1000001$ ($\nu \approx \nu_c - \epsilon^2 = 1/3 - (0.1)^2 = 0.32\bar{3}$)

into nonlinear dynamics, which can be investigated numerically.

We also proposed techniques to improve predictions of solution behavior in the chaotic case. The ensemble method may provide accuracy over long time intervals. Also, given experimental data, statistical procedures can be used to train the model.

Bibliography

[1] Brailovsky, I., and G. Sivashinsky, "Chaotic dynamics in solid fuel combustion", *Physica D* **65** (1993), 191–198.

[2] Danforth, C. M., E. Kalnay, and T. Miyoshi, "Estimating and correcting global weather model error", *Monthly Weather Review* (2006), in press.

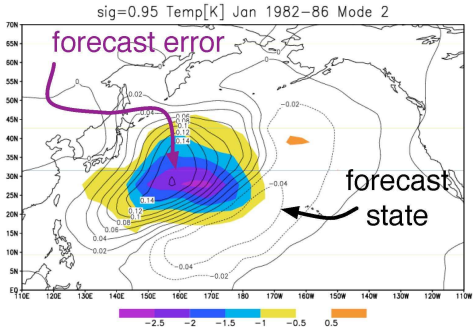

Figure 1.7: Curves of predicted (constant) near sea-surface temperature, along with colored bands of associated error (courtesy of [2])

[3] Frankel, M., V. Roytburd, and G. Sivashinsky, "A sequence of period doubling and chaotic pulsations in a free boundary problem modeling thermal instabilities", *SIAM J. Appl. Math* **54** (1994), 1101–1112.

[4] Gross, L. K., "Weakly nonlinear dynamics of interface propagation", *Stud. Appl. Math.* **108**, 4 (2002), 323–350.

[5] Gross, L. K., and J. Yu, "Weakly nonlinear and numerical analyses of dynamics in a solid combustion model", *SIAM J. Appl. Math* **65**, 5 (2005), 1708–1725.

[6] Matkowsky, B. J., and G. I. Sivashinsky, "Propagation of a pulsating reaction front in solid fuel combustion", *SIAM J. Appl. Math.* **35** (1978), 465–478.

[7] Merzhanov, A. G., "SHS processes: combustion theory and practice", *Arch. Combustionis* **1** (1981), 23–48.

[8] Munir, Z. A., and U. Anselmi-Tamburini, "Self-propagating exothermic reactions: the synthesis of high-temperature materials by combustion", *Mat. Sci. Rep.* **3** (1989), 277–365.

[9] Toth, Z., and E. Kalnay, "Ensemble forecasting at NMC: The generation of perturbations", *Bulletin of the American Meteorological Society* **74**, 12 (1993), 2317–2330.

[10] Yu, J., and L. K. Gross, "The onset of linear instabilities in a solid combustion model", *Stud. Appl. Math.* **107**, 1 (2001), 81–101.